MRS Advances © 2018 Materials Research Society DOI: 10.1557/adv.2018.378

# A Hybrid 3D Printing and Robotic-assisted Embedding Approach for Design and Fabrication of Nerve Cuffs with Integrated Locking Mechanisms

Yuxin Tong, <sup>1</sup> Jamie M. Murbach, <sup>2</sup> Vivek Subramanian, <sup>3</sup> Shrirang Chhatre, <sup>3</sup> Francisco Delgado, <sup>2</sup> David C. Martin, <sup>3</sup> Kevin J. Otto, <sup>2,4</sup> Mario Romero-Ortega, <sup>5</sup> Blake N. Johnson <sup>1,6</sup>

<sup>1</sup>Department of Industrial and Systems Engineering, Virginia Tech, Blacksburg, VA 24061, USA

<sup>2</sup>Department of Biomedical Engineering, University of Florida, Gainesville, FL 32611, USA

<sup>3</sup>Department of Materials Science and Engineering, University of Delaware, Newark, DE 19716, USA

<sup>4</sup>Department of Neuroscience, University of Florida, Gainesville, FL 32611, USA

<sup>5</sup>Department of Bioengineering, University of Texas at Dallas, Richardson, TX 75080, USA

<sup>6</sup>Department of Chemical Engineering, Virginia Tech, Blacksburg, VA 24061, USA. bnj@vt.edu

## ABSTRACT

The ability to interface electronic materials with the peripheral nervous system is required for stimulation and monitoring of neural signals. Thus, the design and engineering of robust neural interfaces that maintain material-tissue contact in the presence of material or tissue micromotion offer the potential to conduct novel measurements and develop future therapies that require chronic interface with the peripheral nervous system. However, such remains an open challenge given the constraints of existing materials sets and manufacturing approaches for design and fabrication of neural interfaces. Here, we investigated the potential to leverage a rapid prototyping approach for the design and fabrication of nerve cuffs that contain supporting features to mechanically stabilize the interaction between cuff electrodes and peripheral nerve. A hybrid 3D printing and robotic-embedding (i.e., pick-and-place) system was used to design and fabricate silicone nerve cuffs (800 µm diameter) containing conforming platinum (Pt) electrodes. We demonstrate that the electrical impedance of the cuff electrodes can be reduced by deposition of the conducting polymer poly(3,4ethylenedioxythiophene) polystyrene sulfonate (PEDOT:PSS) on cuff electrodes via a postprocessing electropolymerization technique. The computer-aided design and manufacturing approach was also used to design and integrate supporting features to the cuff that mechanically stabilize the interface between the cuff electrodes and the peripheral nerve. Both 'self-locking' and suture-assisted locking mechanisms are demonstrated based on the

principle of making geometric alterations to the cuff opening via 3D printing. Ultimately, this work shows 3D printing offers considerable opportunity to integrate supporting features, and potentially even novel electronic materials, into nerve cuffs that can support the design and engineering of next generation neural interfaces.

# INTRODUCTION

Additive manufacturing, commonly referred to as 3D printing, is an emerging computer-aided biomanufacturing process based on the additive assembly of materials.[1,2] Given the principle of the process is based on the robotic-assisted deposition and assembly of materials, 3D printing systems can also be augmented with supporting tools, such as actuators, that support the embedding of pre-fabricated components, commonly referred to as pick-and-place.[3] Furthermore, 3D printing is compatible with the use of medical imaging and computer-aided design approaches for creating digital models (*i.e.*, templates),[4] that serve as the template for tool path data, thereby offering the ability to construct three-dimensional engineered biomimetic systems. As a result, 3D printing is an emerging biomanufacturing process for the design and fabrication of next-generation bioelectronics and biomedical devices.[4-6]

Although multiple types of 3D printing approaches exist, including stereolithography, inkjet printing, microextrusion printing, and laser-assisted bioprinting,[1] microextrusion 3D printing has been widely investigated for the design and fabrication of artificial tissues, biomedical devices, and bioelectronics given its flexibility with a wide range of input materials and material deposition approaches (*e.g.*, jetting or direct filament writing).[2,4-9] For example, microextrusion printing has been used to fabricate vascularized tissues,[10] organs-on-a-chip,[5] and bionics[2,11] based on a wide range of polymeric,[1] electronic,[2] and nanomaterials[2,8,11].

Although 3D printing has been leveraged towards a wide range of applications, it has recently received considerable attention as a potentially disruptive technology in neural engineering, nerve regeneration, and neural interface.[4,5,7,12-14] For example, Johnson et al. showed microextrusion 3D printing can be used to construct compartmentalized microphysiological neural systems-on-a-chip to examine viral transport in the peripheral nervous system. [5,7] Lozano et al. also recently demonstrated that microextrusion 3D printing can be used to construct 3D biomimetic multi-layered brain-like tissues that support the 3D outgrowth of primary cortical neurons.[14] Recently, Johnson et al. also showed microextrusion 3D printing approaches facilitate the fabrication of anatomical bifurcating nerve guidance conduits that contain integrated multi-component gradients of neurotrophic factors.[4] These conduits support the selective regeneration of complex mixed nerve injuries that otherwise would be challenging to repair with conventional nerve repair devices.[4] Here, we show that microextrusion 3D printing can also be leveraged to integrate both electronic materials and supporting mechanical features into conduit architectures to create next-generation cuffs for robust peripheral nerve interface.

#### MATERIALS AND METHODS

Design and 3D Printing of Nerve Cuffs with Integrated Locking Mechanisms: Nerve cuffs were fabricated using a custom microextrusion-based 3D printing system, which consisted of a three-axis robot (MPS75SL; Aerotech), a digital pressure regulator (Ultimus V; Nordson), a motion controller (A3200; Aerotech), and a microscope with a

camera for imaging (OM99-V7; Omano). Design and programming of path information for fabrication of the cuff, embedding of wire electrodes, and integration of locking features was done via manual computer numerical control part programming techniques The bottom half of the 800 µm diameter cuff was first printed using silicone (SI 595CL RTV Silicone; Loctite) at 1.2 mm/s using a 27 gauge tapered tip. The cuff contained two 3D printed perpendicular pathways to support the embedding of cuff electrodes and create interconnects with external conducting wires. A robotic-assisted pick-and-place technique based on an adhesive grasping mechanism was used for embedding of platinum (Pt) wire electrodes (0.25 mm diameter; 99.9%; Alfa Aesar). Prior to embedding, the Pt electrodes were preformed around a rigid 800 µm cylindrical mandrel. Adhesion to the pick-and-place tool was achieved via a silicone-filled 27 gauge The embedded Pt wire was then bonded to a thin copper wire (36 AWG) using a two-part hardener and resin conductive epoxy system (AA-DUCT 907; Atom Adhesives). The interconnect was then insulated via 3D printing of silicone using the aforementioned parameters for connection of the Pt electrodes to the potentiostat. Following insulation, the top half of the cuff was then printed using silicone, which contained either a suture-assisted or self-locking mechanism. Both locking mechanisms were based on the principle of geometric modification of the cuff opening. The sutureassisted locking mechanism consisted of two additional silicone domains added to the middle third of the cuff on both sides of the cuff opening. The self-locking mechanism consisted of a non-linear 'zig-zag' cuff opening. The cuff was then cured at room temperature until the silicone was crosslinked. Deposition of PEDOT:PSS on Cuff Electrodes via Electropolymerization and Measurement of Electrode Impedance: Following fabrication, the cuff was immersed in a

Deposition of PEDOT:PSS on Cuff Electrodes via Electropolymerization and Measurement of Electrode Impedance: Following fabrication, the cuff was immersed in a 1X phosphate buffered saline (PBS) solution containing 0.01M thiophene monomer (3,4-ethylenedioxythiophene; EDOT; 97%; Sigma Aldrich) and 0.1 wt% poly(4-sodium styrene sulfonate) (PSS; M<sub>n</sub> ~ 70,000 g/mol; Sigma Aldrich). The dispersion was prepared by continuous mixing for 2-3 hours. Constant potentiostatic voltage polymerization was performed at 2 V applied to the working electrode (WE) and -2 V applied to the counter electrode (CE) to grow poly(3,4-ethylenedioxythiophene) polystyrene sulfonate (PEDOT:PSS) on the electrode. Polymerization was achieved using a potentiostat (Autolab PGSTAT128N; Metrohm Autolab B.V., Utrecht, Netherlands). Deposition time ranged between 20-60 minutes to vary the PEDOT:PSS deposition. Electrochemical impedance spectroscopy (EIS) measurements were recorded prior to and after polymerization of PEDOT:PSS. EIS measurements were made in 1X PBS over a 0.01-10 kHz frequency range using a 15-sine 25 mV<sub>RMS</sub> excitation voltage.

Interface of 3D Printed Cuff Electrodes with Peripheral Nerve Targets: Validation of 3D printed cuff locking mechanisms was conducted using adult Lewis rats. The sciatic nerve was used for all studies. All procedures were done in strict accordance with good animal practice as defined by the relevant national and local animal welfare bodies, and approved by the University of Florida Institutional Animal Care and Use Committee (IACUC).

As shown in Figure 1, the goal of this study was to demonstrate the ability to design and fabricate nerve cuffs that contain novel supporting features, specifically geometric modifications, that prevent the movement of the electrode-tissue interface during measurement, referred to here as nerve 'locking' mechanisms. Although 3D printing offers the ability to print a wide range of electronic materials,[2,8,11] the creation of a robust neural interface requires strong adhesion between conducting and substrate materials. Thus, we examined a hybrid 3D printing and robotic-assisted embedding process that allowed us to utilize Pt wire electrodes instead of 3D printed conducting materials. This approach enabled us to fabricate nerve cuffs that contained a commonly used high-performance electronic material for neural interface, Pt, while also ensuring strong electrode-substrate adhesion (determined by the extent to which the wire was robotically embedded into the substrate prior to crosslinking).

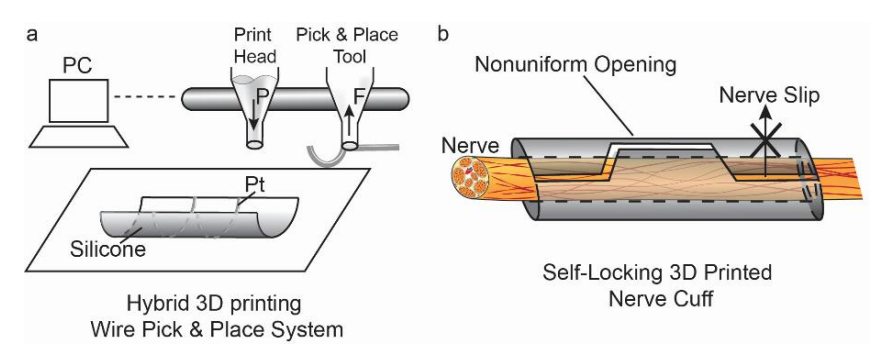


**Figure 1.** Schematic of the hybrid 3D printing and robotic-assisted embedding system (a) and 3D printed nerve cuffs with integrated locking mechanisms (b).

The cuff 3D printing process involved three steps: 1) printing of the bottom half of the cuff; 2) robotic embedding of the wire electrodes; and 3) printing of the top half of the cuff that contained the integrated locking mechanisms. Photographs of nerve cuff throughout the fabrication process are shown in Figure 2. As shown in Figures 2.A and B, we found the ability to robotically embed the wire electrodes in the cuff could be accomplished using an adhesive-based grasping and placement mechanism. The criteria for release of the wire from the pick-and-place tool is that the adhesive force between the wire and the substrate is greater than the adhesive force between the wire and the pick-and-place tool. We found the ratio of these forces could be controlled by two factors: 1) the nozzle size (here a 27 gauge tip) and 2) the depth to which the wire was embedded in the substrate (*i.e.*, the bottom half of the silicone cuff). Photographs of the nerve cuff following the fabrication process are shown in Figures 2.C and D.

The electrical impedance of electrodes used for stimulation and monitoring of peripheral nerve has been shown to be a critical design factor for neural interfaces. For example, the electrical impedance of the device is an important factor associated with the device's power consumption among various other factors. EIS also provides information about the electrode-electrolyte interface. As shown in Figure 2.E, we found that the deposition of PEDOT:PSS on the Pt electrodes led to a reduction in the electrode impedance by approximately two orders of magnitude. Such a result is consistent with previously reported literature.[15-17]

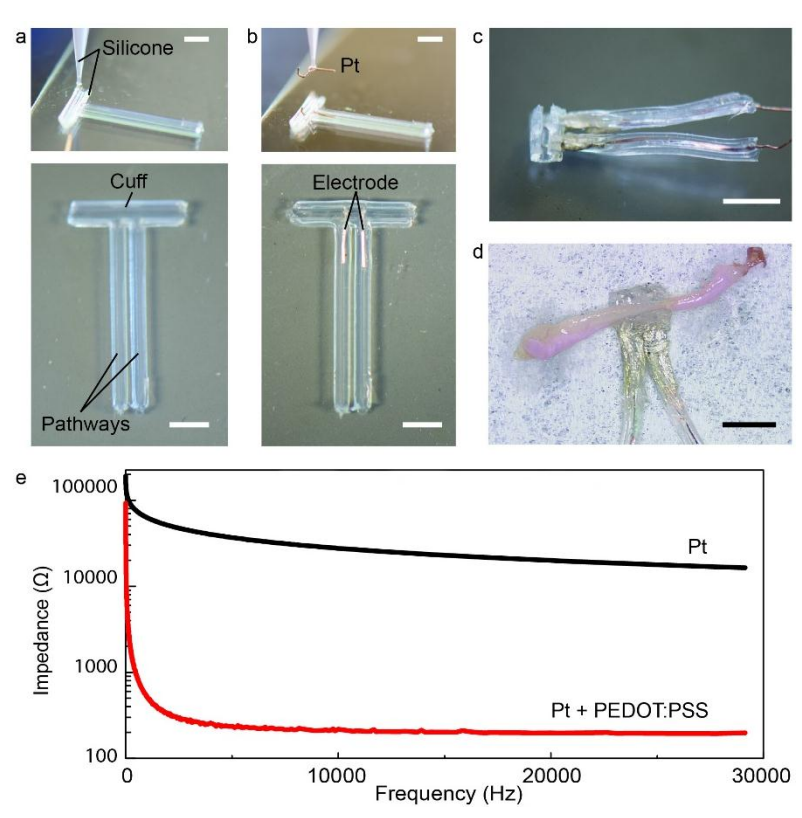
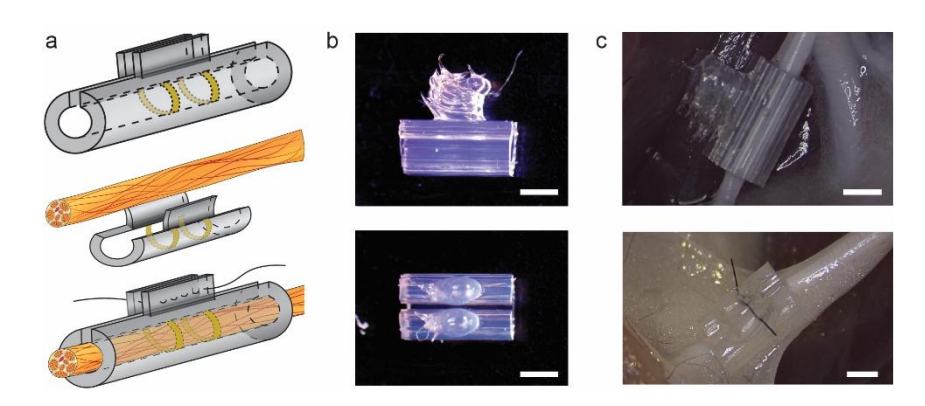


Figure 2. Photographs of the nerve cuff 3D printing process showing: printing of the bottom half of the cuff (a), embedding of the Pt electrode (b), and a fully fabricated nerve cuff (c). d) Insertion of an explanted peripheral nerve in the 3D printed cuff. e) Electrochemical impedance spectrum before and after deposition of PEDOT:PSS. Scale bar = 3 mm.

Having demonstrated that 3D printing can be used to fabricate nerve cuffs that contain robust low impedance Pt-PEDOT:PSS electrodes, we next demonstrated the ability to introduce novel supporting features to the cuff opening that facilitate the ability to retain inserted nerves in the cuff as well as prevent movement of the electrode contact We first examined a suture-assisted locking mechanism. As shown schematically in Figure 3.A, the suture-assisted locking mechanism consisted of two additional silicone domains added to the middle third of the cuff on both sides of the cuff Figure 3.B shows a photograph of a nerve cuff fabricated with the sutureopening. assisted locking mechanism. In vivo implementation showed that the suture-assisted locking mechanism enabled the nerve to be 'locked' in the cuff with a single suture (see Figure 3.C). Importantly, not only did the geometric modification of the cuff opening enable the cuff to be closed using a suture, but it enabled the location of the suturing to be moved away from the nerve, which reduces the risk of accidentally puncturing the nerve or subjecting the nerve to friction from the suture.



**Figure 3.** Schematic (a) and photographs (b) of cuffs with the 3D printed suture-assisted locking mechanism. c) Demonstration of nerve locking capability via *in vivo* implementation. Scale bar = 1 mm.

In addition to the suture-assisted locking mechanisms, it is also of interest to examine alternative locking mechanisms that are suture-free, which we refer to here as 'self-locking' mechanisms. Thus, we next demonstrated the ability to modify the geometric configuration of the cuff opening such that the nerve could be retained in the cuff without the need for suturing. As shown in Figure 4.A, the self-locking mechanism was based on a non-linear cuff opening that exhibited a 'zig-zag' pattern. Figure 4.B shows a photograph of a nerve cuff fabricated with the suture-assisted locking mechanism in both the closed and open figure (accomplished by opening the cuff with a tweezer). Although the self-locking mechanism shown in Figure 4.A and B facilitates the ability to retain nerves in cuffs superior to the retention observed with uniform cuff openings, an important advantage of a 3D printing approach to nerve cuff fabrication is the ability to rapidly prototype designs. This capability is shown in Figure 4.C which shows a self-locking nerve cuff that contains an alternative non-uniform cuff opening, here containing a higher degree of non-uniformity. As shown in Figure 4.D, the nonuniform cuff opening generates two forces that resist nerve slip from the cuff in addition to the normal  $(F_n)$  and frictional  $(F_f)$  forces already present in a traditional cuff that contains a uniform opening  $(F_{cuff})$ . Specifically, the 'flaps' (i.e., the overhanging and interlocking material) present in the self-locking cuffs provide an additional normal force  $(F_{n \, flan})$  to resist nerve slip based on the overhang geometry. Thus, the self-locking cuffs generate an opposing normal force to nerve slip for a longer duration than observed in traditional cuffs with uniform openings. Second, the mechanical contact between the interlocking material (i.e., flaps) creates an additional frictional force ( $F_{fflap}$ ) that resists cuff opening as nerve slip occurs. Overall, this study suggests that non-uniform geometric modifications to cuff designs can provide a useful approach for maintaining electrode-tissue contract for cuffs with extraneural electrode configurations.

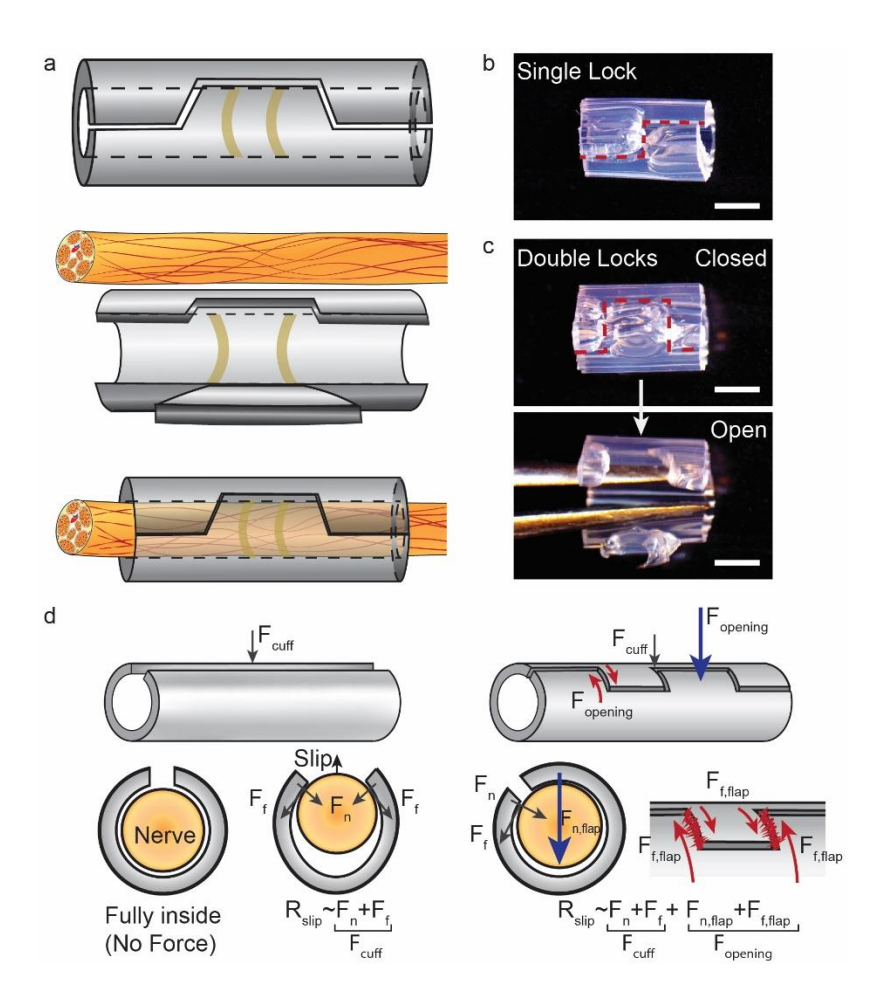


**Figure 4.** Schematic (**a**) and photographs (**b**) of cuffs with the 3D printed self-locking mechanism. **c**) Highlight of a self-locking cuff in a closed and open configuration. **d**) Schematic representation of the additional forces that provide resistance to nerve slip ( $R_{slip}$ ) from self-locking cuffs (traditional cuff – left panel; self-locking cuff – right panel). Scale bar = 1 mm (red dotted lines show the cuff opening).

# **CONCLUSIONS**

Here, we demonstrated the ability to leverage a microextrusion 3D printing and robotic-assisted embedding approach to fabricate nerve cuffs that contain robust low-impedance electrodes composed of Pt and PEDOT:PSS. Importantly, we showed that 3D printing provides the ability to examine non-conventional cuff designs that contain supporting features for retaining nerves after insertion, referred to as 'locking' mechanisms. Multiple types of locking mechanisms were examined based on both suture-based and suture-free approaches. Both mechanisms were based on the ability to modify the geometric configuration of the cuff openings using 3D printing. Ultimately, this work shows that 3D printing offers the ability to fabricate peripheral nerve interfaces that contain supporting mechanisms that may be critical for achieving chronic interfaces with peripheral nerve, especially small diameter nerves and nerve targets that undergo

natural micromotion during testing and usage. Further, the integration of material deposition and embedding approaches into a single 3D printing system also suggests that 3D printing may be used to interface novel electronic materials and electrode configurations with the nervous system.

## References

- 1. S. V. Murphy and A. Atala, Nat. Biotech. 32, 773-785 (2014).
- Y. L. Kong, M. K. Gupta, B. N. Johnson, and M. C. McAlpine, Nano Today 11, 330-350 (2016).
- E. Macdonald, R. Salas, D. Espalin, M. Perez, E. Aguilera, D. Muse and R. B. Wicker, IEEE Access 2, 234-242 (2014).
- B. N. Johnson, K. Z. Lancaster, G. Zhen, J. He, M. K. Gupta, Y. L. Kong, E. A. Engel, K. D. Krick, A. Ju, F. Meng, L. W. Enquist, X. Jia, and M. C. McAlpine, Adv. Funct. Mater. 25, 6205-6217 (2015).
- B. N. Johnson, K. Z. Lancaster, I. B. Hogue, F. Meng, Y. L. Kong, L. W. Enquist, and M. C. McAlpine, Lab Chip 16, 1393-1400 (2016).
- M. Singh, Y. Tong, K. Webster, E. Cesewski, A. P. Haring, S. Laheri, B. Carswell, T. J. O'Brien, C. H. Aardema, R. S. Senger, J. L. Robertson, and B. N. Johnson, Lab Chip 17, 2561-2571 (2017).
- A. P. Haring, H. Sontheimer, and B. N. Johnson, Stem Cell Rev. Rep., 13, 381-406 (2017).
- A. P. Haring, A. U. Khan, G. Liu, and B. N. Johnson, Adv. Opt. Mater. 5, 1700367 (2017).
- M. K. Gupta, F. Meng, B. N. Johnson, Y. L. Kong, L. Tian, Y.-W. Yeh, N. Masters, S. Singamaneni, and M. C. McAlpine, Nano Lett. 15, 5321-5329 (2015).
- H.-W. Kang, S. J. Lee, I. K. Ko, C. Kengla, J. J. Yoo, and A. Atala, Nat. Biotech. 34, 312-319 (2016).
- Y. L. Kong, I. Tamargo, H. Kim, B. N. Johnson, M. K. Gupta, T.-W. Koh, H.-A. Chin,
  D. A. Steingart, B. P. Rand, and M. C. McAlpine, Nano Lett. 14, 7017-7023 (2014).
- B. N. Johnson and X. Jia, Neural Regen. Res. 11, 1568-1569 (2016).
- C. J. Pateman, A. J. Harding, A. Glen, C. S. Taylor, C. R. Christmas, P. P. Robinson, S. Rimmer, F. M. Boissonade, F. Claeyssens, and J. W. Haycock, Biomaterials 49, 77-89 (2015).
- R. Lozano, L. Stevens, B. C. Thompson, K. J. Gilmore, R. Gorkin Iii, E. M. Stewart, M. in het Panhuis, M. Romero-Ortega, and G. G. Wallace, Biomaterials 67, 264-273 (2015).
- K. A. Ludwig, J. D. Uram, J. Yang, D. C. Martin, and D. R. Kipke, J. Neural Eng. 3, 59-70 (2006).
- 16. X. Cui and D. C. Martin, Sens. Actuators B 89, 92-102 (2003).
- 17. S. J. Wilks, A. J. Woolley, L. Ouyang, D.C. Martin, and K. J. Otto, Conf. Proc. IEEE Eng. Med. Biol. Soc., 5412-5415 (2011).